Polymer Journal (2019) 51:989–996
https://doi.org/10.1038/s41428-019-0214-3

FOCUS REVIEW

Mesostructure and orientation control of lyotropic liquid crystals in a polysiloxane matrix

Mitsuo Hara[1]

Received: 29 March 2019 / Revised: 7 May 2019 / Accepted: 8 May 2019 / Published online: 28 May 2019

Abstract

As a preparation method for organic–inorganic or mesoporous inorganic materials via sol–gel condensation of a metal alkoxide, the combination of lyotropic liquid crystals (LLCs) and sol–gel chemistry is a versatile tool to fabricate various nanostructures. Despite previous investigations into such systems, no attempt has been made to utilize the dynamic switching functions of such nanostructures via the phase transition of LLCs in films. A polysiloxane containing an amine-hydrochloride group and a vinyl group was recently synthesized. By controlling the relative humidity, we achieved the phase transition of LLCs and on-demand UV-curing of LLC phases in the polysiloxane film. We further developed vertically oriented organic–inorganic nanochannels by using π−π interactions between discotic molecules and the substrate surface or the spontaneous vertical alignment of LLC containing azobenzene units.

Introduction

Nanostructures and their orientations are important for the functionalization of various materials. The cooperativity of liquid-crystal materials is effective in the preparation of oriented nanostructures on a macroscopic scale, and various studies utilizing these properties are being conducted around the world [1–3]. Of particular note is the use of lyotropic liquid crystals (LLCs) as nanotemplates. As typified by mesoporous silica synthesis, LLC nanostructures and their orientations can be transferred to metal oxides during film formation by combining metal alkoxides with sol–gel methods [4].

The preparation of mesoporous metal oxide materials was first reported in the 1990s [5–8], and hybridization with various metal species and liquid-crystal structures has been attempted [9–12]. There have also been many reports on orientation control methods for nanostructures [13, 14]. The regular nanometer-scale order and macroscopic orientation of nanostructures can be reproducibly transferred to inorganic materials by optimizing the concentration and temperature used when preparing the nanomaterials. However, the environmental responsiveness inherent to LLCs tends to disappear after hybridization with inorganic materials. This is due to the stabilization of the phase by the inorganic materials and solvent evaporation. As such, adjusting the composition of the precursor solution is necessary to change the lyotropic nanostructure and its orientation in prepared organic–inorganic hybrids. Changing the nanostructure or its orientation and immobilizing a specific nanostructure even after organic–inorganic hybridization is a new development in organic–inorganic nanomaterials and LLCs. In particular, phototriggered immobilization [15–18] is easy to apply to the patterning of nanostructures. Furthermore, the processing difficulty of LLC systems, which are difficult to handle due to the presence of the solvent, can be greatly improved. This review focuses on the author's recent developments in the on-demand induction of LLC phase transitions, photofixation methods of LLCs in organic–inorganic hybrid films and vertical alignment techniques of these nanostructures.

Phase transition of LLCs in an inorganic matrix

For phase transitions of LLCs after organic–inorganic hybridization, it is necessary to change the liquid-crystal concentration in the hybrid material. Exposure to solvent vapor can alter the concentration of the composite in the

✉ Mitsuo Hara
mhara@chembio.nagoya-u.ac.jp

[1] Department of Molecular and Macromolecular Chemistry, Graduate School of Engineering, Nagoya University, Furo-cho, Chikusa-ku, Nagoya, Aichi 464-8603, Japan

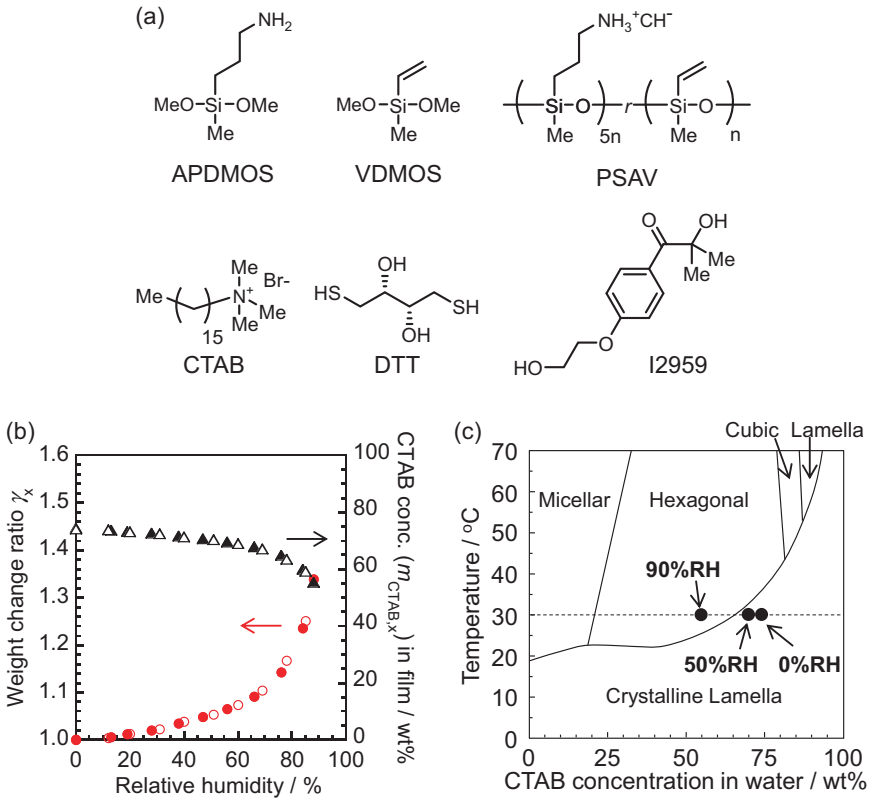

Fig. 1 **a** Chemical structures of the materials used in this section. **b** Weight change ratio (γ_x) of the CTAB-PSAV hybrid film (circle) and CTAB concentration in the film with RH changes (triangle). Filled and open symbols correspond to humidification and dehumidification, respectively. **c** Phase diagram of the CTAB concentrations in the hybrid film at RH = 0%, 50%, and 90%

film while maintaining the film's structure. For example, changing the block copolymer volume fraction by solvent annealing [20], swelling of hydrophilic/hydrophobic phase-separated lamellar structures by humidification [21], or phase transition of ionic supramolecular liquid crystals by humidification [22, 23] have already been reported for this purpose. The author attempted to change the concentration of the LLCs in the inorganic matrix by adjusting the humidity. For this purpose, the author first designed polysiloxane containing hygroscopic and photocrosslinking groups (PSAV in Fig. 1) [19].

PSAV was synthesized through a sol–gel reaction of two types of silane coupling agent (APDMOS and VDMOS). The molar ratio of amine hydrochloride to vinyl groups in PSAV was 5:1, and the molecular weight of PSAV was ~4800 g/mol. The weight of the PSAV as influenced by the relative humidity was measured using a quartz crystal microbalance method. The weight of both the bulk-state PSAV and its spin-cast film (film thickness: ca. 330 nm) increased as the humidity increased. Because polysiloxanes containing amine hydrochloride exhibit hygroscopicity [24], the increase in film weight due to humidity could also be due to the moisture absorption of PSAV. No hysteresis was observed during humidification and dehumidification, and moisture absorption and dehumidification in response to humidity were rapidly repeated. PSAV was very sensitive to ambient humidity. In an organic–inorganic hybrid film consisting of CTAB (as the LLC) and PSAV, the film weight increased as the humidity increased (Fig. 1b). The weight ratio of CTAB to PSAV in the dried film (film at 0% RH) was determined to be ~3:1 based on thermogravimetry (the LC concentration was 75 wt%). The LC concentration in the film at each humidity was calculated from this weight ratio and the amount of moisture absorption; the LC concentration (75 wt%) in the dried film was diluted to 55 wt% at 90% RH (Fig. 1b, triangular plot). Therefore, a liquid-crystal phase transition from lamellar crystals to the hexagonal phase due to humidification is suggested from the CTAB phase diagram [25] (Fig. 1c).

The nanostructures in the hybrid films were evaluated by grazing-incidence X-ray diffraction (GI-XRD) measurements. At 50% RH, a peak with a *d*-spacing of 2.6 nm was observed in the out-of-plane direction of the film. A peak group showing *d*-values of 1/2, 1/3, and 1/4 with respect to the 2.6 nm peak was also observed (Fig. 2a, left). Since various spot-like peaks were observed in the wide-angle region above $2\theta = 15°$, the film structure was judged to be a lamellar crystal structure derived from CTAB. When the hybrid film was exposed to high humidity (90% RH), the diffraction image changed drastically (Fig. 2a, middle). The spacing of the main peak shifted from 2.6 nm to 4.4 nm, and the two-dimensional arrangement pattern of the peaks also changed. Main peaks were observed every 30° in the azimuth direction. A peak of $d = 2.5$ nm was observed

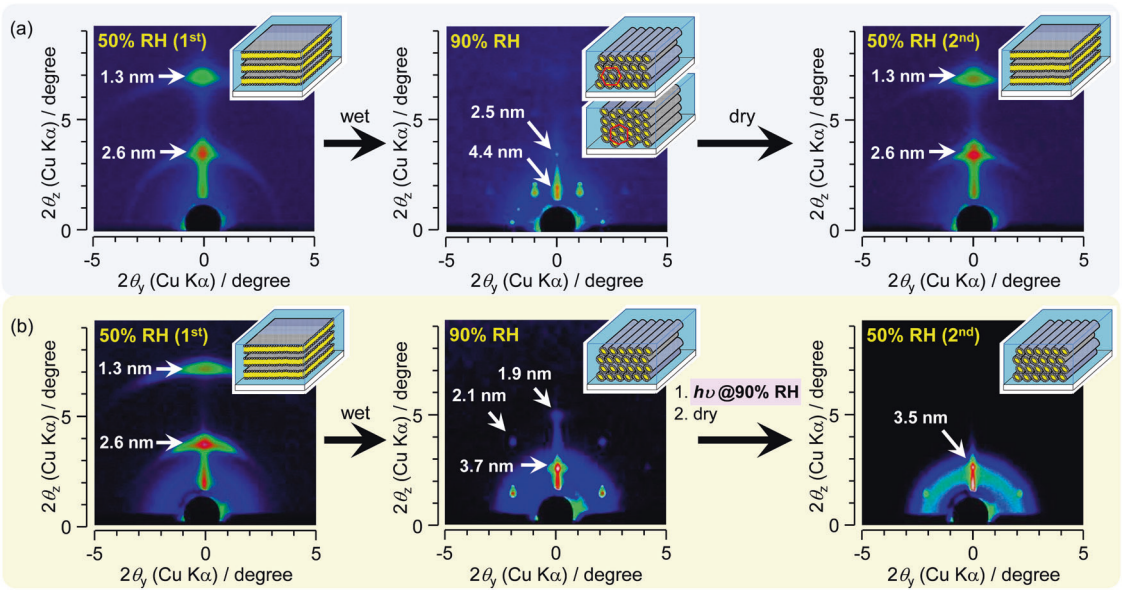

Fig. 2 In situ GI-XRD images and plausible structural models of the CTAB-PSAV hybrid films without (**a**) and with (**b**) DTT and I2959. In (**b**), the right datum was obtained after UV irradiation at 90% RH

immediately on the wide-angle side of the main peak, and the spacing ratio was $1/\sqrt{3}$ with respect to the main peak. In addition, no crystalline peak was observed in the wide-angle range above $2\theta = 15°$, as observed at 90% humidity. Based on these results, CTAB in the hybrid film forms a hexagonal LC phase at 90% humidity. The behavior of this structural change agrees well with the CTAB phase diagram [25], and this phenomenon was not observed in the film consisting solely of CTAB. By hybridizing CTAB with the hygroscopic inorganic material PSAV, an LLC phase transition was induced even after organic–inorganic hybridization. Moreover, this phase transition behavior is reversible (Fig. 2a, right), confirming that CTAB self-assembles based on the relative humidity.

Photofixation of LLC in an inorganic matrix

Similar phase-transition behavior was observed at 50% RH in the composite film consisting of CTAB, PSAV, the crosslinker DTT, and the photoradical generator I2959 (Fig. 2b, left and middle). However, after UV light ($\lambda >$ 310 nm, light intensity at 365 nm: 20 mW cm^{-2}) irradiation of the film at 90% RH, a hexagonal-like diffraction was observed at 50% RH (Fig. 2b, right), showing that the LC phase transition of CTAB was suppressed by UV irradiation. This is because a thiol-ene reaction proceeds between the vinyl group of PSAV and the mercapto group of DTT. Upon dehumidification from 90% to 50%, the disappearance of high-order peaks and a decrease in *d*-spacing were both observed. This could be caused by the shrinkage of the PSAV matrix due to dehumidification and the subsequent decrease in the ordered structure of CTAB.

The phase transition of the lyotropic liquid crystal developed by this method and the process of photofixation are summarized in Fig. 3. At 50% RH and 90% RH, lamellar and hexagonal structures were formed, respectively, and these phase transitions were reversible. However, after UV irradiation at 90% RH, the hexagonal structure was maintained even after dehumidification. As described above, in this method, the LC structure can be converted after film formation, and its structure can be fixed by light. As such, it can be expected that various lyotropic nanostructures can be easily prepared and patterned from one precursor solution composition. This technique can be expanded into easy 1D/2D nanopatterning in organic–inorganic hybrids.

$\pi-\pi$ Interaction-induced vertical alignment

While the cooperative behavior of LC materials is useful for the preparation of nanostructures, another advantage of LC materials is the simple control over the macroscopic orientation of nanostructures [26]. Several methods for controlling the alignment of organic–inorganic nanostructures have been reported by combining LLC and sol–gel methods [13, 14]. Since nanochannels have a large specific surface area, their use as catalyst supports and adsorbents can be developed by controlling their orientation. In particular, vertically aligned nanochannels can be expanded into optical and electrical materials. Various methods have been developed to achieve the vertical alignment of nanochannels, such as film formation using anodized porous alumina [27–29] or grooves [30] prepared by lithography as a template, film formation using the action of magnetic [31, 32]

or electric fields [33, 34], directed evaporation of the solvent during film preparation [35, 36], Stöber solution growth [37], and utilization of structural transitions [38–41]. Examples of vertical alignment by interaction with the substrate interface also exist, such as in film preparation using a chemically neutral interface with a surfactant [42–44] and film preparation using epitaxial growth [45].

In film preparation methods for vertical LLC alignment, the hexagonal phase of typical surfactants, such as CTAB (Fig. 1), Brij® C10, and Pluronic® P-123, can be used as a nanochannel template. The vertical alignment of these surfactants is disadvantageous in terms of free energy, and they undergo no spontaneous vertical alignment. However, the author attempted the vertical alignment of nanochannels by a simple film-forming process based on LLC material design.

Next, the author focused on disc-like molecular materials as LLCs for vertical alignment. Many disc-like molecules can form a columnar LC phase through molecular stacking. In a sandwich cell, this columnar LC phase tends to align perpendicular to the substrate surface [46]. Molecular design guidelines have also been developed that can achieve vertical alignment of the columnar phase with a large area, even if one side is the air interface [47]. The author used a triphenylene derivative, TP (Fig. 4a), as a disc-like molecule exhibiting LLC behavior [48]. Although TP alone forms columnar structures in water, the acceptor molecule TNF was added to improve the stability of the LC phase [49].

TP and TNF were dissolved in a silica precursor solution, and an LLC-silica hybrid film was prepared from this mixture on a silicon wafer surface via heterogeneous nucleation. The film thickness was ~2 μm. Diffraction spots with *d*-spacings of 2 nm were observed in the out-of-plane direction at an azimuth direction of every 60° (Fig. 4b) from GI-XRD measurements. On the wide-angle side, diffraction from the periodic structure of $d = 1.2$ nm was also observed. This result indicates that the hexagonal columnar phase is oriented parallel to the silicon substrate. The same orientation was obtained on quartz glass, and the results did not change even if the wettability of the substrate was changed.

On the other hand, when deposited on the π-conjugated surface of highly ordered pyrolytic graphite (HOPG, GE Advanced Ceramics, STM-1 grade (mosaic spread:

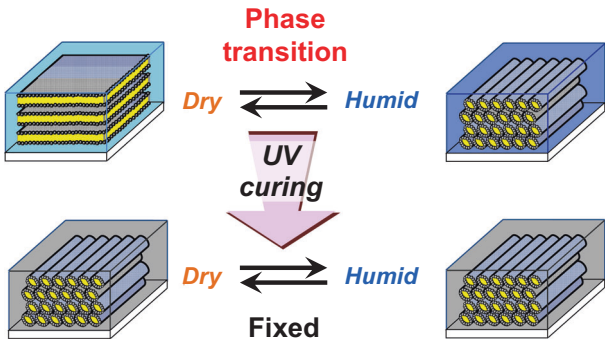

Fig. 3 Schematic illustration of the processes proposed in this work. Experiments were performed in alphabetical order. Yellow and sky-blue regions indicate hydrophobic and hydrophilic parts, respectively

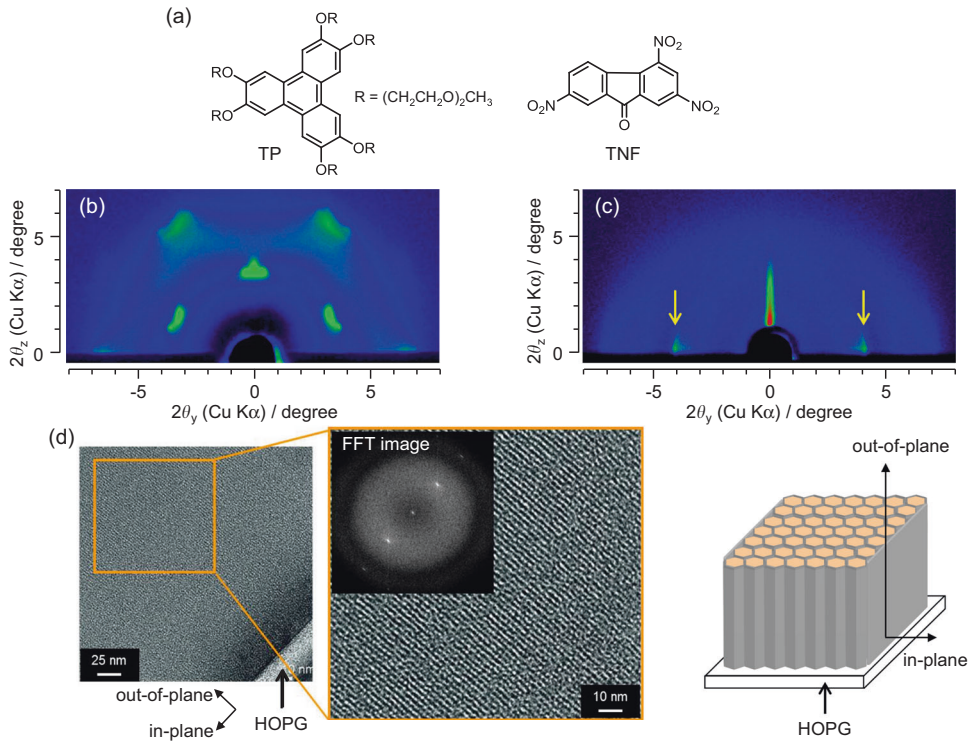

Fig. 4 **a** Chemical structures of the materials used in this section. GI-XRD images taken on imaging plates of the discotic LC-silica films on a Si wafer (**b**) and HOPG (**c**). **d** Cross-sectional TEM image and structural model of the discotic LC/silica hybrid film prepared on HOPG

0.8 ± 0.2°)), diffractions were observed only in the in-plane direction (Fig. 4c). The hexagonal columnar phase was judged to be vertically aligned with the substrate. From the cross-sectional transmission electron microscopy (TEM) image of the film, a vertical stripe pattern with a width of ~2 nm was observed in the out-of-plane direction, revealing the existence of a vertically aligned columnar structure on the substrate interface (Fig. 4d). Since the hexagonal phases of CTAB and P123 are aligned parallel to the substrate even on HOPG, the vertical alignment on HOPG is specific to a discotic LLC with a π-conjugate plane. It is noteworthy that the vertical alignment, which can range in thickness to several micrometer, is governed by the π−π interaction at the substrate interface.

In the case of vertically aligned nanostructures on HOPG, the discotic LLC was removed by calcination at 500 °C or by photolysis. The in-plane scattering peak intensity increased after calcination, which is due to the increase in the density difference of electrons in the periodic structure of the film, suggesting the formation of a porous structure. Thus, a simple preparation method for vertically aligned nanoporous silica films was developed by utilizing the interaction between the substrate surface and LC molecules.

Spontaneous vertical alignment on a universal substrate

The vertical alignment approach using disc-like LLC molecules limits the applicable substrate to HOPG. Here, the author focused on the vertical alignment of a microphase-separated structure in a thermotropic LC azobenzene block copolymer. Thermotropic liquid crystalline azobenzene block copolymers can induce vertical alignment of azobenzene molecules containing groups such as polyethylene oxide blocks [51–53] or polystyrene blocks [54]. Depending on the alignment, the cylindrical microphase separation structure is also vertically oriented. In particular, since amphiphilic block copolymers undergo hydrophilic–hydrophobic phase separation, the formation of a self-assembled structure in water and the appearance of LLC behavior can also be expected [50].

In this study, the amphiphilic diblock copolymer PMEO-*b*-PAz (Fig. 5a) was synthesized by a two-step atom transfer radical polymerization method. The weight fraction of the PAz block in PMEO-*b*-PAz, denoted as ϕ_{Az}, was 0.55. As a result of differential scanning calorimetry measurements, polarization microscope observations, and SAXS measurements of the bulk sample, the thermophysical properties of PMEO-*b*-PAz were characterized as glass (below 57 °C), smectic C (57–95 °C), smectic A (95–104 °C), and isotropic (above 104 °C), showing thermotropic liquid crystallinity. The azobenzene mesogen in the spin-cast film of PMEO-*b*-PAz was vertically aligned to the substrate by annealing at a temperature above the isotropic point. Moreover, adding water to PMEO-*b*-PAz increased the microphase-separated period and showed a negative correlation with ϕ_{Az}. Based on this result, PMEO-*b*-PAz is a unique material with a thermotropic and lyotropic LC nature.

To prepare a hybrid film of PMEO-*b*-PAz and silica, PMEO-*b*-PAz was added to a silica precursor solution, and the mixture solution was spin-cast onto a quartz glass or

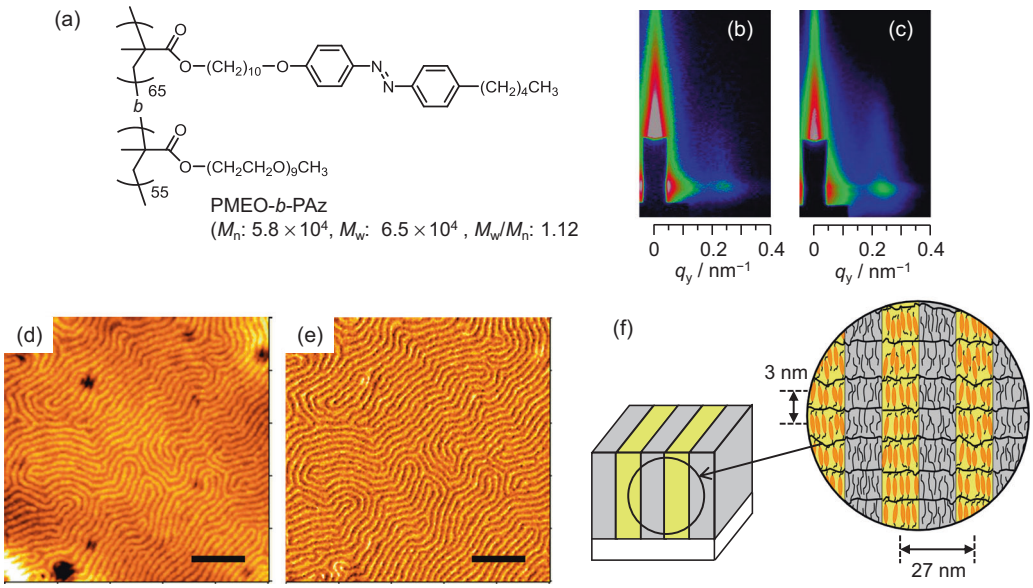

Fig. 5 **a** Chemical structures of the materials used in this section. GI-SAXS images taken on imaging plates of the PMEO-*b*-PAz/silica films **b** before and **c** after photodecomposition. **d** Topographical and **e** phase-contrast AFM images of films after photodecomposition (scale bar: 200 nm). **f** Plausible model of the hybrid film

silicon wafer. The thickness of the spin-cast film was ca. 120 nm. After annealing the film, scattering derived from the ~27 nm periodic structure was observed only in the in-plane direction based on GI-SAXS measurements (Fig. 5b). In the GI-SAXS measurements with the wide-angle region as the detection target, 3-nm-period scattering was observed only in the out-of-plane direction. From the SAXS measurement results of the bulk sample, the length of 27 nm is close to the microphase-separated period of PMEO-*b*-PAz, and the period of 3 nm agrees well with the layer spacing of the smectic phase formed by azobenzene. That is, the microphase-separated structure is aligned perpendicular to the substrate. However, in the film without annealing, scattering of the smectic phase was not detected. Therefore, it can be inferred that the vertical alignment of the microphase-separated structure of PMEO-*b*-PAz is induced by the orientation of the smectic phase in the PAz block (Fig. 5f).

After UV-ozone treatment was applied to the hybrid film, the scattering in the in-plane direction became clearer (Fig. 5c). An atomic force microscope (AFM) image of the film surface showed a stripe morphology equal to the microphase-separated period. These results suggest that the organic component was removed from the film by UV-ozone treatment. It is possible to confirm from the phase image that the stripe pattern is continuous inside the hole, even though it appears the same as the hole in the AFM topographical image (Fig. 5d, e). That is, the stripe image is derived from the vertically aligned lamellar structure. By utilizing the spontaneous vertical orientation of PMEO-*b*-PAz, the author developed a new preparation method for vertically aligned nanoporous silica films. Of particular note is the simplicity of this process. Since there is no need for substrate pretreatment and no restriction on the type of substrate that can be used, the fact that vertically aligned silica nanostructures can be obtained by only annealing after spin-casting is an attractive element for the application of nanomaterials.

This method can also make the inorganic elements present relatively easy to customize. The author also examined the combination of this method with titanium-based inorganic substances. A spin-cast film was prepared from a mixture of a titanium-based sol and PMEO-*b*-PAz, and subsequent calcination was performed to obtain a vertically aligned nanoporous film with anatase crystalline titania as a matrix (pore diameter: ca. 20 nm). This film showed almost 100% transmittance in the visible region. When a vertically aligned nanoporous titania film in which the sensitizing dye N719 had been introduced into the nanopores was used as a titania electrode for a dye-sensitized solar cell (DSSC), power was generated under irradiation with artificial sunlight (AM1.5, 1SUN). The conversion efficiency from light energy to electric power was very low (0.04%), but when converted to the amount of unit dye introduced, the conversion efficiency was ~1.5 times higher than that of the control electrode consisting of a titania nanoparticle film. Although many studies are still needed to optimize the cell parameters, including the film thickness, dye introduction method, DSSC cell assembly, and current–voltage measurement conditions, to the results present an example of the utility of vertically aligned nanoporous structures.

Chromonic LCs

By focusing not only on the nanostructures of LLCs but also on their functionality due to their molecular structure, it may be possible to prepare useful materials without removing the template. The author would like to introduce the importance of focusing on the molecular functions of LLCs, which is outside the topic of vertical alignment [55, 56].

There is a group of compounds that absorb in the visible region and show LLC nature, referred to as chromonic LCs [57, 58]. LLC phases of general-purpose molecules such as CTAB have frequently been used as templates for the synthesis of nanoporous silica, but attempts to use a chromonic LC phase as a template have not been published. Stabilization of the alignment-controlled chromonic LC phase with inorganic materials is expected to create new organic–inorganic composite nanomaterials that retain the optical properties of the chromonic LC.

The chromonic LC B67 (Fig. 6) is a disc-like molecule, and the molecules stack face-to-face to form a discotic columnar LC phase in water [59]. A mixed solution consisting of B67 and silica sol was spin-cast onto quartz glass and a hybrid film with a thickness of ca. 650 nm was prepared. However, the absorption spectrum revealed that the B67 in the film was in a different aggregation state from that in water, and the process did not lead to the immobilization of the lyotropic columnar phase with silica. As a result of detailed analysis, it became clear that the film had a lamellar structure in which B67 layers and silica layers were alternately laminated. This lamellar structure is a novel structure for B67 and is a very interesting finding. It is inferred that the less-polar B67 cannot form a columnar phase in the sol as the solvent evaporates during the film-forming process, and finally, the B67 layer and the silica layer undergo phase separation and structural transformation into a lamellar structure. In addition, electrostatic repulsion between anionic B67 and the negatively charged silica matrix is a factor in the phase separation. To allow B67 columns to stably form in concentrated silica sol, 2-(2-aminoethoxy)ethanol (AEE) was added to the precursor solution to act as a mediator molecule at both interfaces. As a result, the compatibility between the B67 column and the silica sol

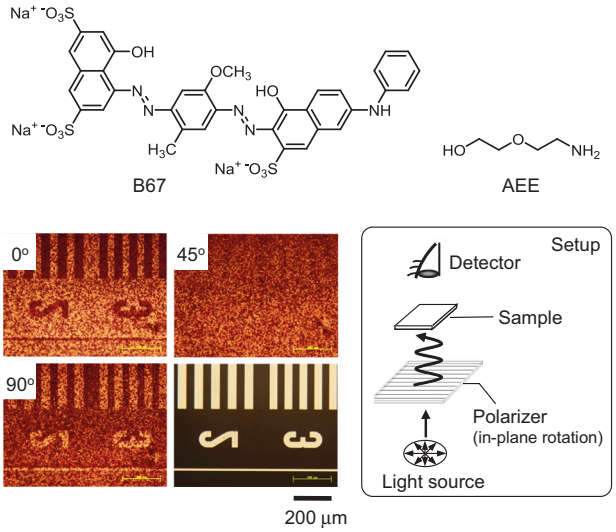

Fig. 6 Optical microscopy images of B67-silica film and photomask observed with polarized incident light. The angles in each image indicate the polarization direction of incident light

was improved, and immobilization of the columnar phase with silica was achieved.

In a B67-silica hybrid film prepared by dip-coating, the columnar structure was aligned parallel to the dipping direction of the substrate, and the film showed absorption anisotropy. This alignment was induced by the solution flow when pulling up the substrate. In addition, micropatterning of the columnar phase was achieved by combining photoalignment and flow orientation (Fig. 6). This patterning was maintained above the isotropic point of B67 because it was stabilized by the inorganic compound. The absorption anisotropy of the columnar phase was used more effectively by controlling the orientation of the B67 columnar LC phase than just fixing it.

Summary and outlook

In this review, the author describes a method to control the on-demand phase transition and alignment of organic–inorganic hybrid containing LLCs. First, the author developed polysiloxanes with hygroscopicity and photocrosslinking groups. In mixed films of polysiloxane and LLCs, the phase transition of the LLC can be induced by changes in humidity, and the phase-transition behavior can be suppressed by light irradiation. In a system using triphenylene derivatives, the author proposed a new method for vertically aligning nanochannels by preparing a film on a HOPG substrate. By using an amphiphilic diblock copolymer with vertical alignment ability, spontaneous vertical alignment was achieved without substrate restrictions. The results also suggest that the vertically aligned nanostructure has the potential to be useful as an electrode for dye-sensitized solar cells. In the system using chromonic LCs, optical functional behavior was shown by the material without removing the template. Thus, the cooperative behavior of the LLC materials works effectively to control the formation and orientation of nanostructures in the macroscopic region. The LLC-handling process described in this review is expected to be part of next-generation nanotechnology.

Acknowledgements This work was supported in part by a Grant-in-Aid for Early-Career Scientists (No. 18K14283) and Young Scientists (B) (No. 25810117) of the Japan Society for the Promotion of Science. The author expresses sincere gratitude to Professor Takahiro Seki, Professor Yukikazu Takeoka, and Professor Shusaku Nagano for their continuous and kind guidance, to all collaborators, and particularly to the students for their great contributions.

Compliance with ethical standards

Conflict of interest The authors declare that they have no conflict of interest.

Publisher's note: Springer Nature remains neutral with regard to jurisdictional claims in published maps and institutional affiliations.

References

1. Kato T, Yoshio M, Ichikawa T, Soberats B, Ohno H, Funahashi M. Nat Rev Mater. 2017;2:17001.
2. Seki T, Nagano S, Hara M. Polymer. 2013;54:6053.
3. Zhao Y, Ikeda T, editors. Smart light-responsive materials. New Jersey: John Wiley & Sons 2009.
4. Lu GQ, Zhao XS, editors. Nanoporous materials: science and engineering. London: Imperial College Press; 2004. vol. 4.
5. Kresge CT, Leonowicz ME, Roth WJ, Vartuli JC, Beck JS. Nature. 1992;359:710.
6. Beck JS, Vartuli JC, Roth WJ, Leonowicz ME, Kresge CT, Schmitt KD, et al. J Am Chem Soc. 1992;114:10834.
7. Inagaki S, Fukushima Y, Kuroda K. J Chem Soc Chem Commun. 1993; 680–82. https://doi.org/10.1039/C39930000680
8. Inagaki S, Koiwai A, Suzuki N, Fukushima Y, Kuroda K. Bull Chem Soc Jpn. 1996;69:1449.
9. Simon PFW, Ulrich R, Spiess HW, Wiesner U. Chem Mater. 2001;13:3464.
10. Wan Y, Zhao D. Chem Rev. 2007;107:2821.

11. Ariga K, Vinu A, Yamauchi Y, Ji Q, Hill JP. Bull Chem Soc Jpn. 2012;85:1.
12. Innocenzi P, Malfatti L. Chem Soc Rev. 2013;42:4198.
13. Innocenzi P, Malfatti L, Kidchob T, Falcaro P. Chem Mater. 2009;21:2555.
14. Stein A, Rudisill SG, Petkovich ND. Chem Mater. 2014;26:259.
15. Gin DL, Gu W, Pindzola BA, Xhou W-J. Acc Chem Res. 2001;34:973.
16. Wiesenauer BR, Gin DL. Polym J. 2012;44:461.
17. Yang J, Wegner G. Macromolecules. 1992;25:1786.
18. Yang J, Wegner G. Macromolecules. 1992;25:1791.
19. Hara M, Orito T, Nagano S, Seki T. Chem Commun. 2018;54:1457.
20. Sinturel C, Vayer M, Morris M, Hillmyer MA. Macromolecules. 2013;46:5399.
21. Krishnan K, Iwatsuki H, Hara M, Nagano S, Nagao Y. J Mater Chem A. 2014;2:6895.
22. Zhang H, Li L, Möller M, Zhu X, Hernandez JJ, Rosenthal M, et al. Adv Mater. 2013;25:3543.
23. Chen Y, Lingwood MD, Goswami M, Kidd BE, Hernandez JJ, Rosenthal M, et al. J Phys Chem B. 2014;118:3207.
24. Kaneko Y, Toyodome H, Shoiriki M, Iyi N. Int J Polym Sci. 2012; 684278 14.
25. Auvray X, Petipas C, Anthore R, Rico I, Lattes A. J Phys Chem. 1989;93:7458.
26. Hara M, Nagano S, Seki T. J Am Chem Soc. 2010;132:13654.
27. Yamaguchi A, Uejo F, Yoda T, Uchida T, Tanamura Y, Yamashita T, et al. Nat Mater. 2004;3:337.
28. Platschek B, Petkov N, Himsl D, Zimdars S, Li Z, Köhn R, et al. J Am Chem Soc. 2008;130:17362.
29. Yamauchi Y, Nagaura T, Inoue S. Chem Asian J. 2009;4:1059.
30. Wu C-W, Ohsuna T, Edura T, Kuroda K. Angew Chem Int Ed. 2007;46:5364.
31. Tolbert SH, Firouzi A, Stucky GD, Chmelka BF. Science. 1997;278:264.
32. Yamauchi Y, Sawada M, Sugiyama A, Osaka T, Sakka Y, Kuroda K. J Mater Chem. 2006;16:3693.
33. Walcarius A, Sibottier E, Etienne M, Ghanbaja J. Nat Mater. 2007;6:602.
34. Vilà N, Ghanbaja J, Aubert E, Walcarius A. Angew Chem Int Ed. 2014;53:2945.
35. Zhang Y, Wang J. J Am Ceram Soc. 2010;93:365.
36. Shan F, Lu X, Zhang Q, Wu J, Wang Y, Bian F, et al. J Am Chem Soc. 2012;134:20238.
37. Teng Z, Zheng G, Dou Y, Li W, Mou C-Y, Zhang X, et al. Angew Chem Int Ed. 2012;51:2173.
38. Wu C-W, Ohsuna T, Kuwabara M, Kuroda K. J Am Chem Soc. 2006;128:4544.
39. Koh C-W, Lee U-H, Song J-K, Lee H-R, Kim M-H, Suh M, et al. Chem Asian J. 2008;3:862.
40. Ko Y-S, Koh C-W, Lee U-H, Kwon Y-U. Microporous Mesoporous Mater. 2011;145:141.
41. Oveisi H, Jiang X, Imura M, Nemoto Y, Sakamoto Y, Yamauchi Y. Angew Chem Int Ed. 2011;50:7410.
42. Chen B-C, Lin H-P, Chao M-C, Mou C-Y, Tang C-Y. Adv Mater. 2004;16:1657.
43. Freer EM, Krupp LE, Hinsberg WD, Rice PM, Hedrick JL, Cha JN, et al. Nano Lett. 2005;5:2014.
44. Koganti VR, Dunphy D, Gowrishankar V, Mcgehee MD, Li X, Wang J, et al. Nano Lett. 2006;6:2567.
45. Richman EK, Brezesinski T, Tolbert SH. Nat Mater. 2008;7:712.
46. Monobe H, Awazu K, Shimizu Y. Adv Mater. 2006;18:607.
47. Kajitani T, Fukushima T. Ekisho. 2014;18:139.
48. Boden N, Bushby RJ, Hardy C, Sixl F. Chem Phys Lett. 1986;123:359.
49. Bengs H, Ebert M, Karthaus O, Kohne B, Praefcke K, Ringsdorf H, et al. Adv Mater. 1990;2:141.
50. Hara M, Nagano S, Seki T. Bull Chem Soc Jpn. 2013;86:1151.
51. Yu HF, Kobayashi T. ACS Appl Mater Interface. 2009;1:2755.
52. Asaoka S, Uekusa T, Tokimori H, Komura M, Iyoda T, Yamada T, et al. Macromolecules. 2011;44:7645.
53. Komiyama H, Iyoda T, Kamata K. Chem Lett. 2012;41:110.
54. Morikawa Y, Kondo T, Nagano S, Seki T. Chem Mater. 2007;19:1540.
55. Hara M, Nagano S, Mizoshita N, Seki T. Langmuir. 2007;23:12350.
56. Hara M, Nagano S, Kawatsuki N, Seki T. J Mater Chem. 2008;18:3259.
57. Lydon J. J Mater Chem. 2010;20:10071.
58. Lydon J. Curr Opin Colloid Interface Sci. 2004;8:480.
59. Ruslim C, Matsunaga D, Hashimoto M, Tamaki T, Ichimura K. Langmuir. 2003;19:3686.

Mitsuo Hara is an assistant professor of Graduate School of Engineering in Nagoya University. In 1982, he was born in Aichi, Japan. He worked at FUJIFILM Corporation in 2007–2009, and he was a JSPS Research Fellow in 2010–2012. He received Ph.D. in 2012 from Nagoya University under the supervision of Professor Takahiro Seki. In 2012, he started an academic carrier at Nagoya University. His current research interests includes molecular self-assembly systems and surface alignment of organic–inorganic hybrids containing lyotropic liquid crystals. He received Award for Encouragement of Research in Liquid Crystal Science from the Japanese Liquid Crystal Society (2014), Award for Encouragement of Research in Polymer Science from the Society of Polymer Science, Japan (2018), and Best Poster Award at 27th Polymer Material Forum, the Society of Polymer Science, Japan (2018).